Journal of Food Science and Technology (Iran)

Homepage:www.fsct.modares.ir

Scientific Research

Nano-Enhanced Antifungal and Antimycotoxigenic Activity of Ethanolic Extract of *Ganoderma lucidum* Against Mycotoxigenic Fungi

Muna J. N. Al-Tamimi[1]*, Ban M. H. Al-Zobaidy[1]

1-Department of Biology, College of Education for Pure Sciences, University of Karbala, Iraq

ARTICLE INFO

Article History:

Received: 2026/05/04
Review: 2026/05/13
Accepted: 2026/06/07

Keywords:
Ganoderma lucidum,
Mycotoxins,
Nano-formulation,
Ethanolic extract,
Antifungal activity,
HPLC,
Mycotoxin inhibition,
Nanotechnology

DOI: 10.48311/fsct.2026.120269.83131

*Corresponding Author E-Mail:
muna.j@s.uokerbala.edu.iq

ABSTRACT

The problem of mycotoxin contamination is considered one of the key threats to food safety, agricultural production, and public health worldwide. The current study aimed at exploring the antifungal and antimycotoxigenic properties of Ganoderma lucidum ethanolic extract (GLEE) and its nano-formulated version towards mycotoxigenic fungi in legumes, cereals, and nuts. Thirteen mycotoxigenic fungi, comprising such genera as Aspergillus, Penicillium, Fusarium, and Alternaria, have been isolated by employing both morphological and molecular approaches, Aspergillus flavus being predominant in composition. The nano-formulation of GLE was based on the value of the minimum fungicidal concentration (MFC) of the crude extract (2.5 mg/mL). According to the data obtained, the MIC value of GLE was 2 mg/mL and the MFC value amounted to 2.5 mg/mL, while the application of nano-formulation caused a decrease in those parameters to 0.5 mg/mL and 1 mg/mL, correspondingly. Moreover, the HPLC analysis revealed an evident drop in the level of mycotoxin synthesis in the samples under investigation. It can be concluded that nano-formulation leads to an increase in the antifungal and antimycotoxigenic effects of Ganoderma lucidum extracts. Thus, nano-formulated G. lucidum can be regarded as a potentially useful approach to mycotoxigenic fungi control.

1- INTRODUCTION

Mycotoxins are toxic secondary metabolites secreted by various filamentous fungi of genera such as *Aspergillus*, *Penicillium*, *Fusarium*, and *Alternaria*. They occur in agricultural products such as cereals, legumes, and nuts, thus presenting serious risks to food safety as well as the health of animals and humans. Chronic consumption of mycotoxins leads to adverse impacts on human health such as hepatotoxicity, immunosuppression, carcinogenicity, and endocrine disruption [1]. The global prevalence of mycotoxin contamination in staple food commodities underscores the urgent need for effective, safe, and sustainable control strategies.

The persistence of mycotoxins under varied environmental conditions, as well as their stability during food processing, makes them a significant challenge when using physical and chemical treatments for their control. Consequently, more emphasis has been placed on exploring natural methods, especially bioactive compounds from medicinal plants and fungi, which are safer, efficient, cost-effective, eco-friendly, and do not compromise food safety [2]. Recent research has increasingly focused on plant- and fungal-derived bioactive compounds as alternative antifungal and antimycotoxigenic agents, aligning with consumer demand for clean-label food preservation methods [3].

Ganoderma lucidum is an edible medicinal fungus whose bioactivity has drawn much attention due to its composition of many bioactive compounds, such as triterpenoids, polysaccharides, phenolics, and sterols. These bioactive compounds possess various biological properties, including antioxidant, antifungal, and antimicrobial activities. Previous studies have reported that extracts of *G. lucidum* exhibit antifungal activity and can disrupt the mycotoxin biosynthesis pathway [3]. However, the specific bioactive constituents responsible for antimycotoxigenic activity and their mechanisms of action require further elucidation.

One of the most common techniques for acquiring bioactive compounds is ethanolic extraction, owing to its effectiveness in isolating both polar and non-polar bioactive molecules. However, the efficacy of the biological functions of crude extracts is limited by issues such as poor solubility, limited stability, and restricted access to microbial cells. Furthermore, batch-to-batch variability in extract composition poses challenges for reproducibility and standardization. The utilization of nano-sciences could help address some of these challenges.

Nanotechnology has proven to enhance the biological performance of natural extracts by increasing their surface area, improving solubility, and facilitating absorption by microorganisms [4]. Moreover, nanotechnology enhances the biological activity of extracts by enabling the regulated delivery of bioactive compounds, thus improving antifungal activity and reducing toxin production. Green synthesis of metal and metal oxide nanoparticles, particularly zinc oxide nanoparticles (ZnO-NPs), is highly effective due to the combined antifungal mechanisms of the nanoparticles themselves (membrane disruption, reactive oxygen species

generation, and intracellular damage) and the bioactive coating from the extract [5].

Despite these advances, studies providing a direct comparative evaluation of crude and green-synthesized nano-formulated extracts of *Ganoderma lucidum* against mycotoxigenic fungi isolated from diverse food sources (cereals, legumes, and nuts) remain limited. Moreover, there is insufficient information regarding the simultaneous assessment of fungal growth inhibition and mycotoxin reduction—two distinct but interconnected biological effects—achieved through nano-formulation. The distinction between growth-dependent and growth-independent inhibition of mycotoxin production is critical for establishing true antimycotoxigenic activity.

Therefore, the present study aims to (1) evaluate and compare the antifungal activity of ethanolic and green-synthesized ZnO-nano-formulated extracts of *Ganoderma lucidum* against mycotoxigenic fungi isolated from selected food commodities, (2) assess and distinguish the antimycotoxigenic efficacy of these treatments using HPLC quantification, and (3) comprehensively characterize the nano-formulation to substantiate claims of nano-scale enhancement. This study tests the hypothesis that the green-synthesized ZnO nano-formulation of *Ganoderma lucidum* extract enhances both antifungal and antimycotoxigenic efficacy compared to the conventional ethanolic extract, through the synergistic interaction of bioactive compounds and ZnO nanoparticles.

2-Materials and Methods

Preparation of Ethanolic Extract of *Ganoderma lucidum*

Ganoderma lucidum fruiting bodies were obtained and authenticated taxonomically. The material was dried in an air drier at 40°C and milled to a fine powder (particle size < 0.5 mm). The powder was macerated with 70% (v/v) ethanol at a ratio of 1:10 (w/v) under constant agitation on an orbital shaker at 150 rpm for 72 hours at room temperature (25 ± 2°C). The macerated material was filtered through Whatman No. 1 filter paper. The filtrate was concentrated using a rotary evaporator under reduced pressure at 45°C to remove the solvent [5]. The resulting crude extract was stored at 4°C in amber glass vials until further use. The extraction yield was calculated as the ratio of dried extract weight to initial powder weight (%, w/w). Standardization was performed by quantifying total phenolic content using the Folin-Ciocalteu method to ensure batch consistency for biological assays.

Green Synthesis of Zinc Oxide Nanoparticles (ZnO-NPs)

The synthesis of ZnO nanoparticles was performed using a green chemistry approach, wherein the ethanolic extract of *Ganoderma lucidum* served as both the reducing agent (converting Zn^{2+} to ZnO) and the capping/stabilizing agent (preventing agglomeration). The minimum fungicidal concentration (MFC = 2.5 mg/mL) of the ethanolic extract was selected as the basis for nanoparticle formulation to ensure that any enhancement over the crude extract could be attributed to

nano-scale effects rather than simply increased concentration. Zinc acetate dihydrate [$Zn(CH_3COO)_2 \cdot 2H_2O$, 0.1 M] was dissolved in deionized water and added dropwise to the extract solution under continuous magnetic stirring at 600 rpm. The reaction mixture was maintained at 70 ± 5°C with the pH adjusted to 9.0 using 0.1 M NaOH for 2–3 hours. Formation of ZnO nanoparticles was visually indicated by a progressive color change from pale yellow to a creamy white precipitate. The resulting nanoparticles were collected by centrifugation at 10,000 rpm for 15 minutes, washed three times with deionized water and once with ethanol to remove unreacted precursors, and dried in a hot air oven at 60°C for 12 hours. The dried nanoparticles were stored in airtight containers at room temperature until characterization and biological testing [6].

Source and Identification of Fungi

Fifty samples of visibly mold-contaminated food commodities, including cereals (wheat, maize, rice), legumes (chickpeas, lentils, beans), and nuts (peanuts, almonds, pistachios), were collected from local markets in the Basra region, Iraq. Fungal isolates were obtained by direct plating of surface-disinfected samples onto Potato Dextrose Agar (PDA) supplemented with chloramphenicol (50 mg/L) to suppress bacterial growth. Plates were incubated at 25°C for 5–7 days, and emerging fungal colonies were purified by hyphal tip transfer. Identification was performed using both morphological/microscopic characteristics (colony morphology, conidial structures, and sporulation patterns) with reference to standard taxonomic keys and molecular identification. For molecular confirmation, the internal transcribed spacer (ITS) region of ribosomal DNA was amplified using universal primers ITS1 and ITS4, and the sequences were compared with the NCBI GenBank database using BLAST analysis. Thirteen mycotoxigenic fungal isolates were identified, comprising *Aspergillus flavus* (2 isolates), *A. fumigatus*, *A. oryzae*, *A. versicolor*, *Penicillium chrysogenum*, *P. citrinum*, *P. glabrum*, *P. odoratum*, *P. thomii*, *Fusarium falciforme*, *Alternaria alternata*, and *A. porri*.

Antifungal Activity Assay

The antifungal efficacy of the ethanolic extract and ZnO nanoparticles was evaluated using the radial growth inhibition assay on Potato Dextrose Agar (PDA). Sterilized PDA medium was amended with the extract or nanoparticles to achieve final concentrations of 0.5, 1.0, 1.5, 2.0, and 2.5 mg/mL before solidification. Fungal discs (5 mm diameter) from 7-day-old actively growing cultures were inoculated at the center of each plate. Control plates contained PDA without any treatment. Plates were incubated at 26 ± 1°C for 7 days. Fungal growth was recorded by measuring the colony diameter (mm) in two perpendicular directions, and the mean was calculated. The percentage of growth inhibition was calculated using the formula: Inhibition (%) = [(C − T) / C] × 100, where C is the colony diameter of the control and T is the colony diameter of the treatment. All experiments were performed in triplicate (n = 3).

Determination of Minimum Inhibitory Concentration (MIC) and Minimum Fungicidal Concentration (MFC)

MIC was determined as the lowest concentration at which no visible fungal growth was observed after 7 days of incubation. For MFC determination, fungal discs from plates showing complete inhibition (MIC and higher) were sub-cultured onto fresh, treatment-free PDA plates and incubated for an additional 7 days. MFC was defined as the lowest concentration at which no fungal growth was observed on the recovery plates, indicating fungicidal rather than fungistatic activity. The assays were performed in triplicate.

GC–MS Analysis

The ethanolic extract of *Ganoderma lucidum* was analyzed by gas chromatography-mass spectrometry (GC–MS) using a Shimadzu QP2010 Ultra system (Japan). Chromatographic separation was performed with an Rtx-5MS capillary column (30 m × 0.25 mm × 0.25 µm film thickness). Helium (99.999% purity) was used as carrier gas at a flow rate of 1 mL/min. The oven temperature program started at 60°C for 2 min, followed by a ramp of 10°C/min to 280°C, held for 10 min. The injector temperature was 250°C, operated in split mode (1:50), and the ion source temperature was 200°C. The instrument was operated in electron ionization (EI) mode at 70 eV. Identification of bioactive compounds was accomplished by comparing mass spectra with the NIST14 and Wiley11 spectral libraries.

HPLC Analysis of Phenolic Compounds

The phenolic profile of the ethanolic extract was analyzed by high-performance liquid chromatography (HPLC) using a Shimadzu LC-20AT system (Japan) equipped with a UV–Visible detector. Separation was performed on a C18 column (250 × 4.6 mm, 5 µm particle size). The mobile phase consisted of methanol:water (with 0.1% formic acid) in a ratio of 70:30 (v/v) under isocratic elution. The flow rate was 1 mL/min, injection volume was 20 µL, and detection was performed at 280 nm. Quantification of individual phenolic compounds (caffeic acid, ferulic acid, gallic acid, hydrobenzoic acid, quercetin, rutin, and ganoderic acid A) was performed using external calibration curves prepared from authentic standards. Results were expressed as µg of compound per mg of extract.

Spectroscopic Analysis (UV–Vis and FTIR)

The UV–Vis absorption spectra of the ethanolic extract and ZnO nanoparticles were recorded using a Shimadzu UV-1800 spectrophotometer (Japan) in the wavelength range of 200–800 nm, with quartz cuvettes of 1 cm path length. Deionized water and ethanol were used as blanks for nanoparticles and extracts, respectively. FTIR spectra were recorded using a PerkinElmer Spectrum Two FTIR spectrophotometer (USA) in the wavenumber range of 400–4000 cm^{-1} at a resolution of 4 cm^{-1}, using the KBr pellet method.

X-ray Diffraction (XRD) Analysis

The crystalline structure of the ZnO nanoparticles was analyzed by X-ray diffraction using a Bruker D8 Advance diffractometer (Germany) in the

2θ range of 10°–80° with Cu Kα radiation (λ = 1.5406 Å) at 40 kV and 40 mA. The average crystallite size was calculated using the Debye–Scherrer equation: $D = K\lambda / (\beta \cos \theta)$, where K is the shape factor (0.9), λ is the X-ray wavelength, β is the full width at half maximum (FWHM) in radians, and θ is the Bragg diffraction angle.

Microscopic Analysis (SEM, TEM, and EDX)

The morphological features and particle size of the nanoparticles were characterized by scanning electron microscopy (SEM; JEOL JSM-IT500, Japan) at an accelerating voltage of 15 kV. Samples were sputter-coated with gold prior to imaging. The internal structure and size distribution of the nanoparticles were determined by transmission electron microscopy (TEM; JEOL JEM-2100F, Japan) at 200 kV. Samples were prepared by drop-casting a diluted nanoparticle suspension onto carbon-coated copper grids and air-drying. Energy dispersive X-ray (EDX) analysis was performed in conjunction with SEM to determine the elemental composition and purity of the synthesized ZnO nanoparticles.

TEM Analysis of Treated Fungal Cells

To visualize the effect of treatments on fungal ultrastructure, hyphal samples from control and treated cultures (at MIC concentrations) were fixed in 2.5% glutaraldehyde in 0.1 M phosphate buffer (pH 7.2), post-fixed in 1% osmium tetroxide, dehydrated in a graded ethanol series, embedded in epoxy resin, sectioned, and examined by TEM.

Mycotoxin Extraction and Quantification by HPLC

For the assessment of antimycotoxigenic activity, *Aspergillus flavus* (the predominant aflatoxin producer among the isolates) was cultured in YES (Yeast Extract Sucrose) broth supplemented with treatments at sub-inhibitory concentrations (0.5 × MIC) to separate effects on growth from effects on toxin biosynthesis. Following incubation at 26°C for 10 days, aflatoxin B1 was extracted using liquid-liquid extraction with chloroform. The extract was evaporated to dryness under nitrogen and reconstituted in methanol. Mycotoxin quantification was performed by HPLC (Shimadzu LC-20AT) with fluorescence detection (excitation: 365 nm, emission: 435 nm) after post-column derivatization using a Kobra cell. Separation was achieved on a C18 column with a mobile phase of water:acetonitrile:methanol (60:25:15, v/v/v) at 1 mL/min. Quantification was based on external calibration with certified aflatoxin B1 standards. Results were expressed as parts per billion (ppb).

Statistical Analysis

Statistical analysis was performed using SPSS version 25. Data are presented as mean ± standard deviation (SD) of three independent replicates (n = 3). One-way analysis of variance (ANOVA) followed by Duncan's multiple range test or least significant difference (LSD) was used to compare treatment means. Differences were considered statistically significant at $p \leq 0.05$.

3-Results and Discussion

GC–MS Analysis of Ethanolic Extract

The GC–MS analysis of the ethanolic extract of *Ganoderma lucidum* identified twenty-five (25) compounds with high similarity indices (≥ 85%) against the NIST database. The chromatogram revealed peaks at various retention times, demonstrating the chemical complexity of the extract (Fig. 1). The identified compounds were categorized into distinct chemical classes including phenolic compounds, fatty acids, fatty acid esters, cyclic compounds, and terpenoids. Notably, eugenol (2.62%), anethole (1.54%), and estragole were the major phenolic constituents, while oleic acid (collectively ≈ 30% across multiple peaks), n-hexadecanoic acid (2.82%), and octadecenoic acid ethyl ester (8.47%) constituted the dominant fatty acid fraction. Squalene (9.87%), a triterpenoid known for its bioactive properties, was the most abundant terpenoid identified. The presence of these bioactive compounds provides a chemical basis for the observed antifungal and antimycotoxigenic activities, as phenolics are known membrane disruptors and fatty acids can interfere with fungal signaling pathways [7]. A comprehensive list of identified compounds is presented in Table 1.

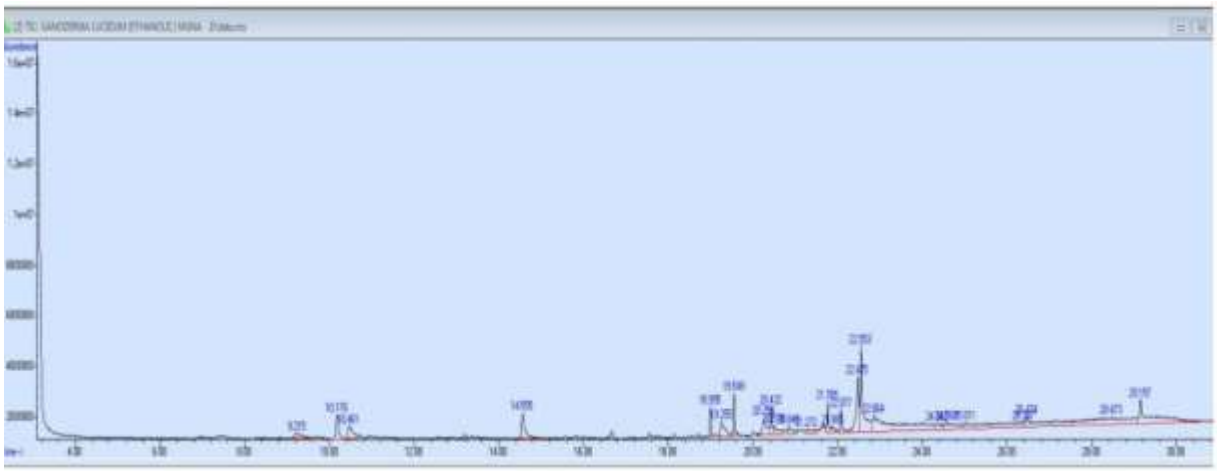

Figure (1): GC-MS Chromatogram of ethanol extract of Ganoderma lucidum

Table (1): Identified compounds by GC–MS with retention time and percentage

No.	Chemical Classification	Relative Abundance (%)	Retention Time (min)	Compound Name
1	Phenolic compounds	1.54	9.215	Anethole
2	Cyclic compounds	2.61	10.176	Cyclohexene derivative
3	Phenolic compounds	2.62	10.461	Eugenol
4	Esters	2.90	14.555	Diethyl phthalate
5	Cyclic compounds	1.58	18.995	Naphthalene derivative
6	Nitrogen-containing compounds	2.79	19.255	Benactyzine
7	Fatty acid esters	2.18	19.549	Hexadecanoic acid methyl ester
8	Fatty acids	2.82	20.259	n-Hexadecanoic acid
9	Esters	1.69	20.432	Hexadecanoic acid ethyl ester

10	Fatty acids	1.72	20.510	n-Hexadecanoic acid
11	Organic compounds	1.27	20.848	Disparlure
12	Fatty acids	1.20	21.272	Tetradecanoic acid
13	Fatty acid esters	1.87	21.765	Octadecenoic acid methyl ester
14	Fatty acids	1.09	21.886	Oleic acid
15	Esters	1.63	22.077	Methyl stearate
16	Fatty acid esters	5.90	22.475	Isopropyl linoleate
17	Fatty acid esters	8.47	22.553	Octadecenoic acid ethyl ester
18	Fatty acids	14.72	22.864	Oleic acid / Eicosanoic acid
19	Fatty acids	1.40	24.362	Oleic acid
20	Fatty acids	2.89	24.569	Oleic acid
21	Fatty acids	1.72	25.011	Oleic acid
22	Fatty acids	6.69	26.387	Oleic acid
23	Fatty acids	4.52	26.473	Oleic acid
24	Fatty acids	14.31	28.473	n-Decanoic acid
25	Terpenoid compounds	9.87	29.157	Squalene

HPLC Analysis of Phenolic Compounds

Quantitative HPLC analysis identified and quantified seven phenolic compounds in the ethanolic extract (Table 2). Ganoderic acid A, a triterpenoid specific to Ganoderma species, was the most abundant compound (485.7 µg/mg extract), followed by gallic acid (269.8 µg/mg), rutin (214.9 µg/mg), and quercetin (198.0 µg/mg). Caffeic acid (65.9 µg/mg), ferulic acid (92.6 µg/mg), and hydrobenzoic acid (74.0 µg/mg) were present at lower but significant concentrations. The high concentration of ganoderic acid A is particularly noteworthy, as triterpenoids from G. lucidum have been previously associated with antimicrobial and enzyme-inhibitory activities. The presence of quercetin and gallic acid, both well-documented antioxidants and membrane-active compounds, supports the proposed mechanisms of antifungal action involving membrane disruption and oxidative stress [10,11]. The chromatographic data with standard comparisons are shown in Figures 2–8.

29/10/2025 01:20 pm Chromatogram F:\ sample .PRM Page 1 of 1

Chromatography Laboratory
HPLC

Sample Info:

Sample ID	: sample	Amount	0
Sample	: sample	ISTD Amount	0
Inj. Volume [mL]	: 0.1	Dilution	1

Autostop	: 20.00 min	External Start	: Start - Restart, Down
Detector 1	: Detector 3	Range 1	: Bipolar, 2000 mAU, 10 Sample. per Sec.
Subtraction Chromatogram	: (None)	Matching	: No Change

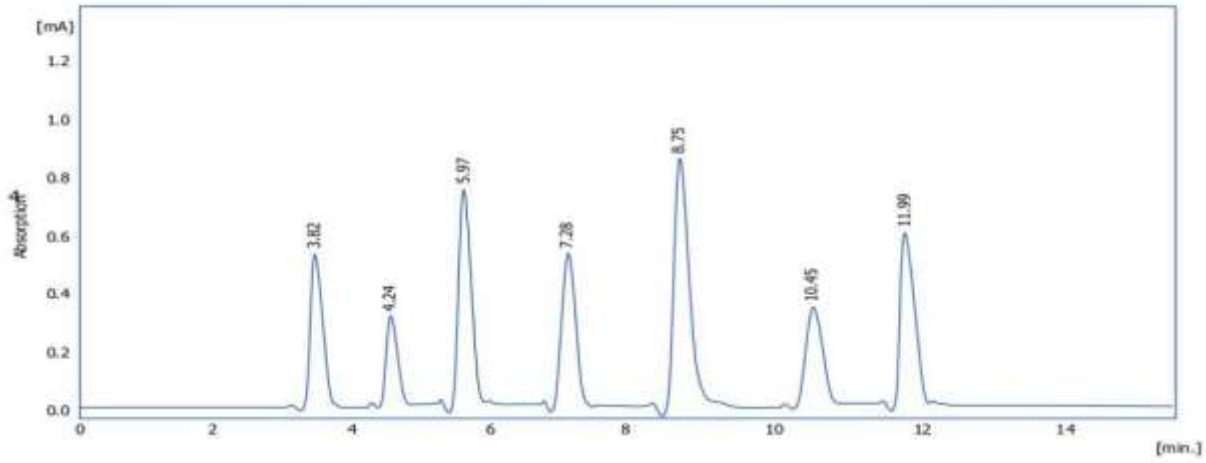

Result chromatography Table (Uncal - F:\ sample)

No	Reten. Time [min]	Area [mAU.s]	Height [mAU]	Area [%]	Height [%]	W05 [min]	Compound Name
1	3.82	12056.00	574.59	14.00	14.00	0.08	
2	4.24	8520.12	322.65	9.00	9.00	0.05	
3	5.97	16332.09	784.14	18.00	18.00	0.10	
4	7.28	13245.06	562.54	14.00	14.00	0.08	
5	8.75	19887.04	806.54	21.00	21.00	0.15	
6	10.45	8544.14	265.41	9.00	9.00	0.05	
7	11.99	12665.00	544.14	15.00	15.00	0.08	
	Total	84521.96	3860.52	100.00	100.00		

Fig. (2): HPLC chromatogram of ethanolic extract

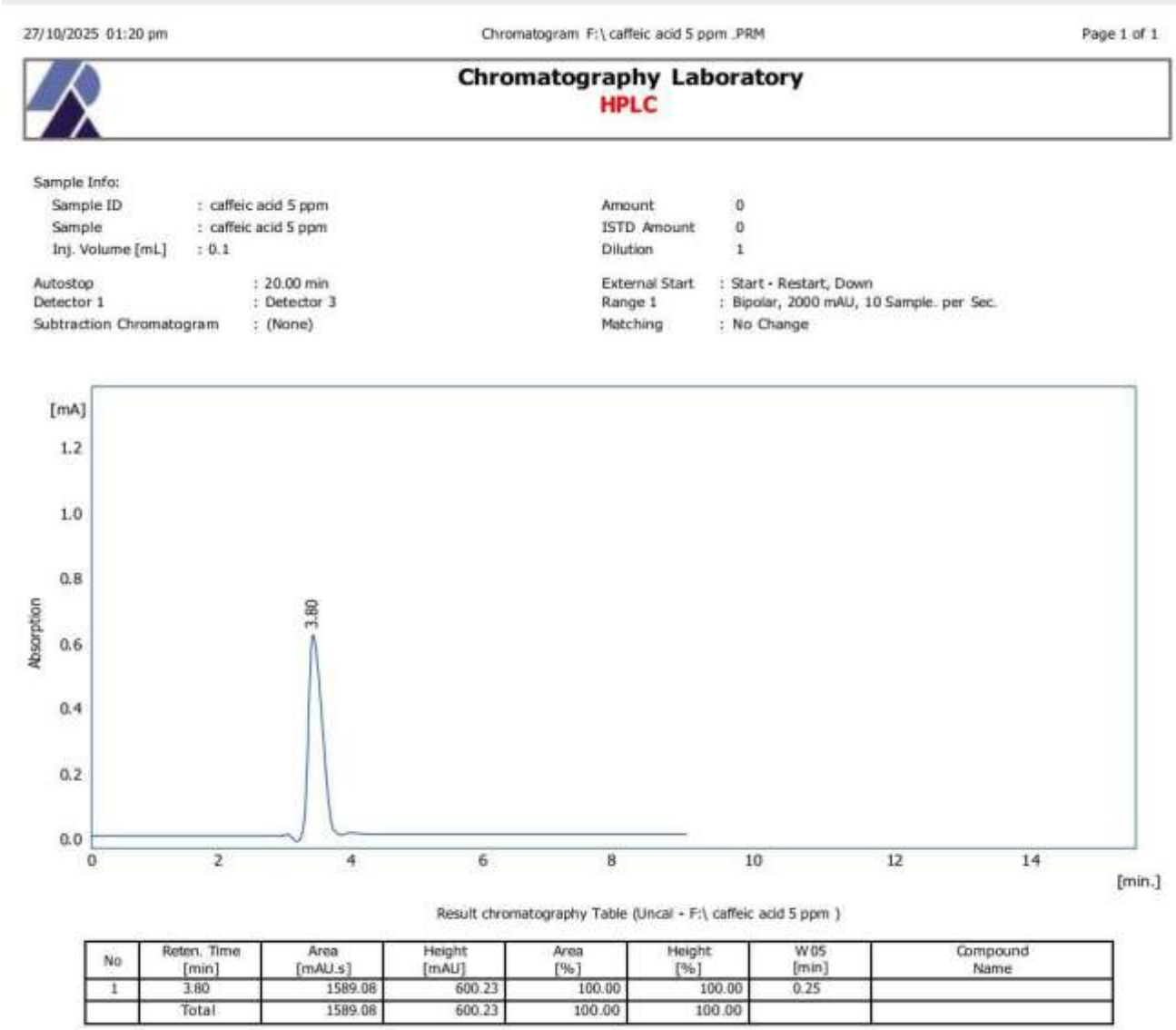

No	Reten. Time [min]	Area [mAU.s]	Height [mAU]	Area [%]	Height [%]	W 05 [min]	Compound Name
1	3.80	1589.08	600.23	100.00	100.00	0.25	
	Total	1589.08	600.23	100.00	100.00		

Fig. 3. Standard chromatogram of Caffeic acid.

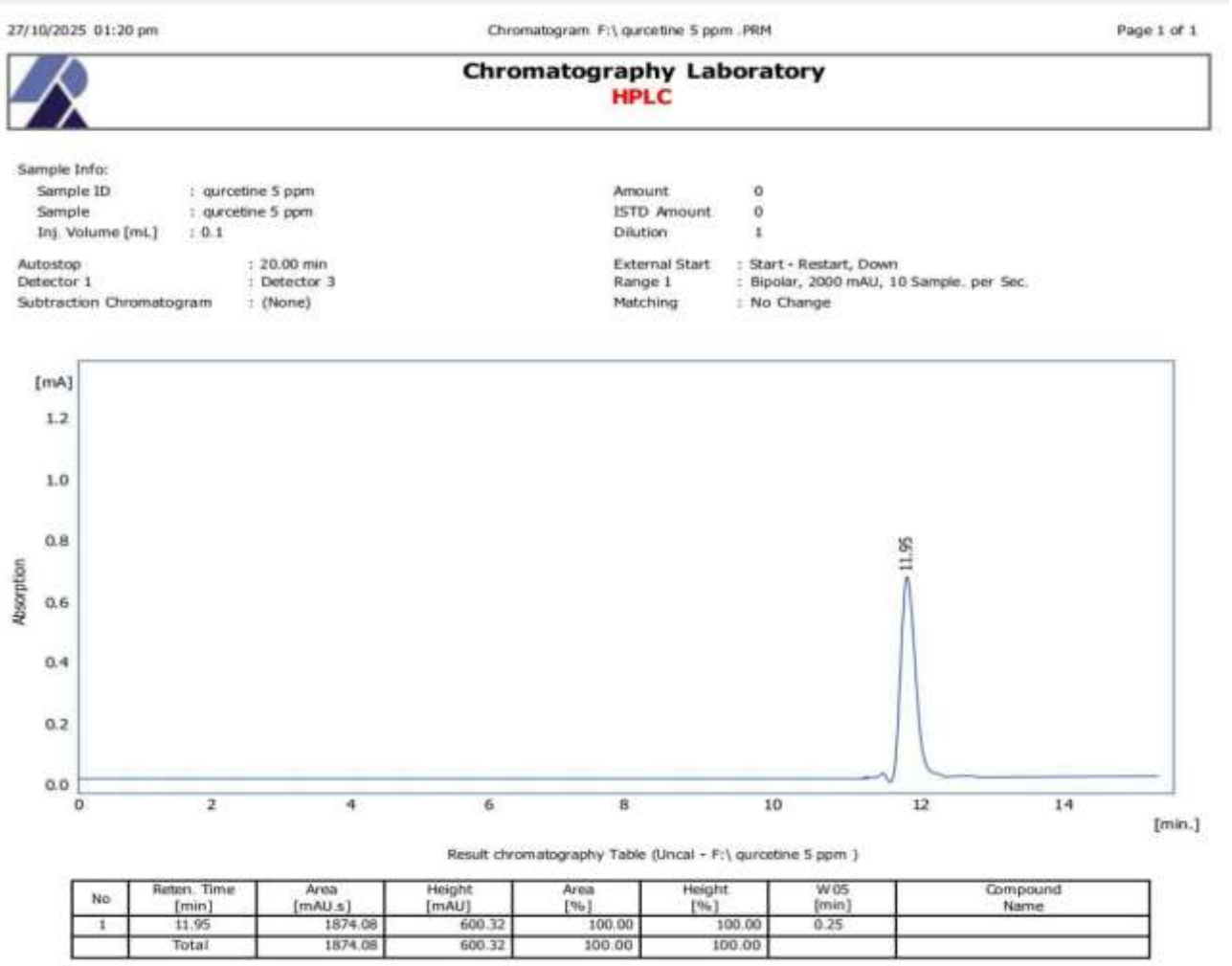

No	Retten. Time [min]	Area [mAU.s]	Height [mAU]	Area [%]	Height [%]	W05 [min]	Compound Name
1	11.95	1874.08	600.32	100.00	100.00	0.25	
	Total	1874.08	600.32	100.00	100.00		

Figure 4 . Standard chromatogram Quercetin

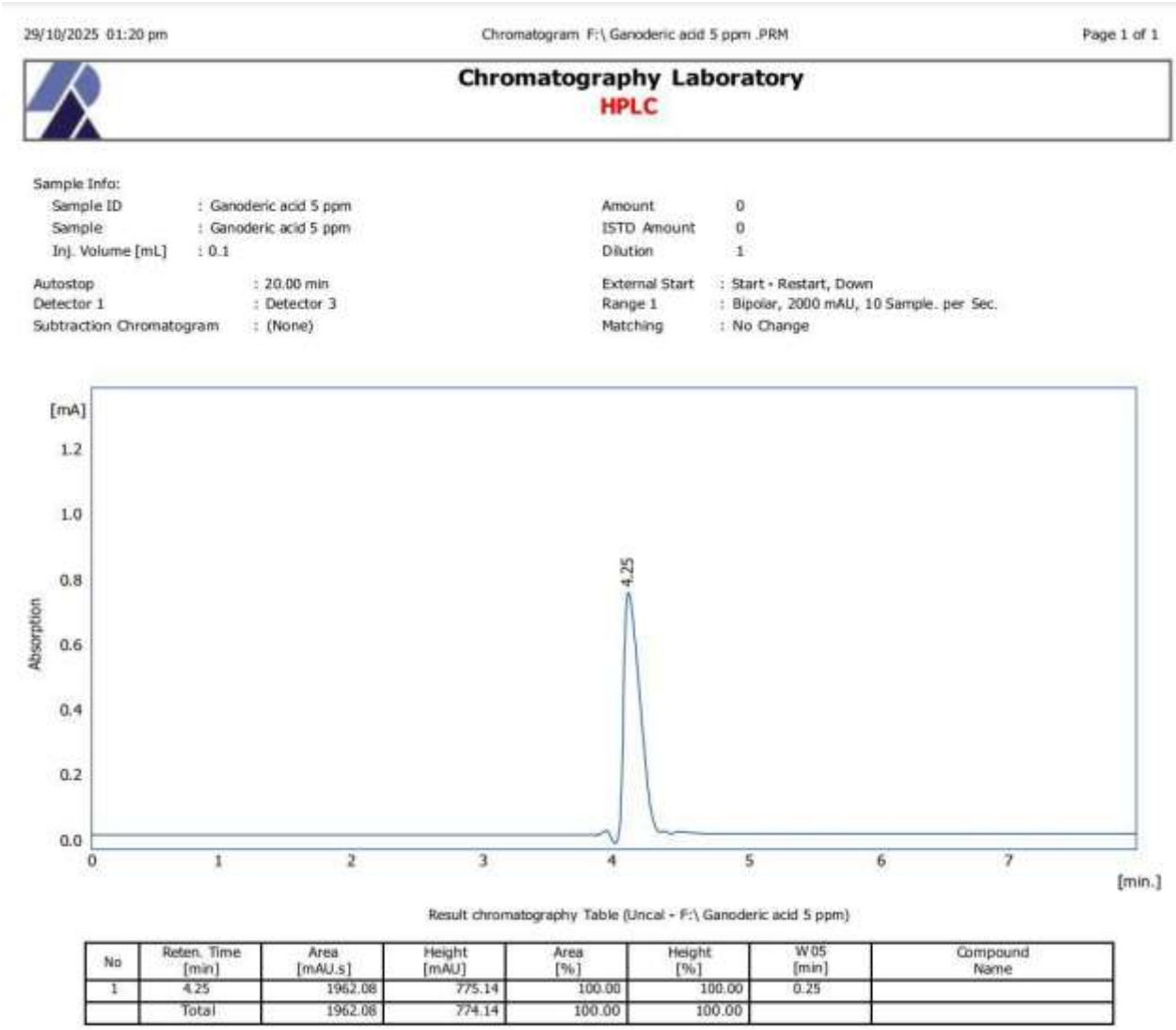

Result chromatography Table (Uncal - F:\ Ganoderic acid 5 ppm)

No	Reten. Time [min]	Area [mAU.s]	Height [mAU]	Area [%]	Height [%]	W05 [min]	Compound Name
1	4.25	1962.08	775.14	100.00	100.00	0.25	
	Total	1962.08	774.14	100.00	100.00		

Figure 5. Standard chromatogram Ganoderic acid

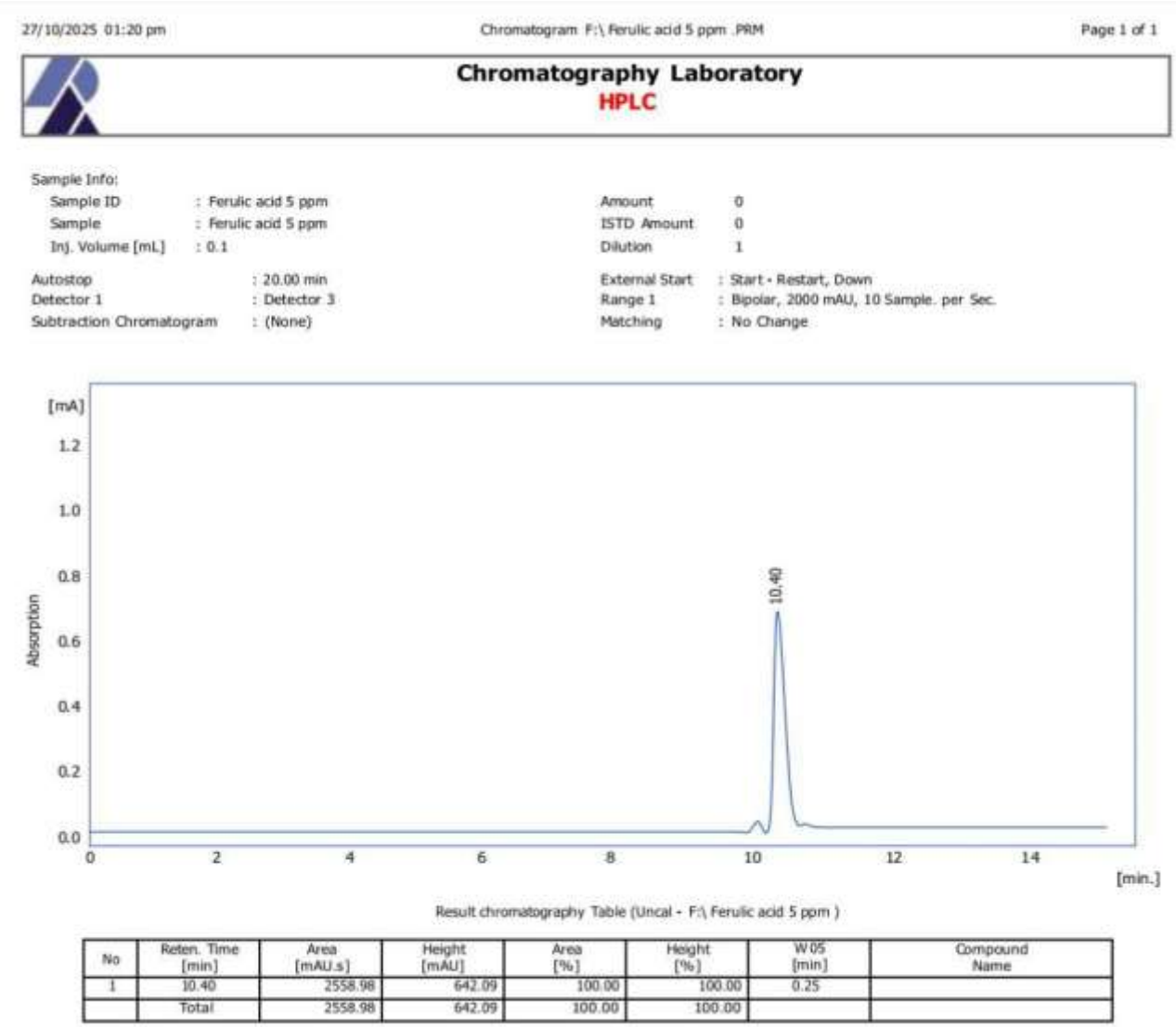

Result chromatography Table (Uncal - F:\ Ferulic acid 5 ppm)

No	Reten. Time [min]	Area [mAU.s]	Height [mAU]	Area [%]	Height [%]	W 05 [min]	Compound Name
1	10.40	2558.98	642.09	100.00	100.00	0.25	
	Total	2558.98	642.09	100.00	100.00		

Figure 6. Standard chromatogram Ferulic acid

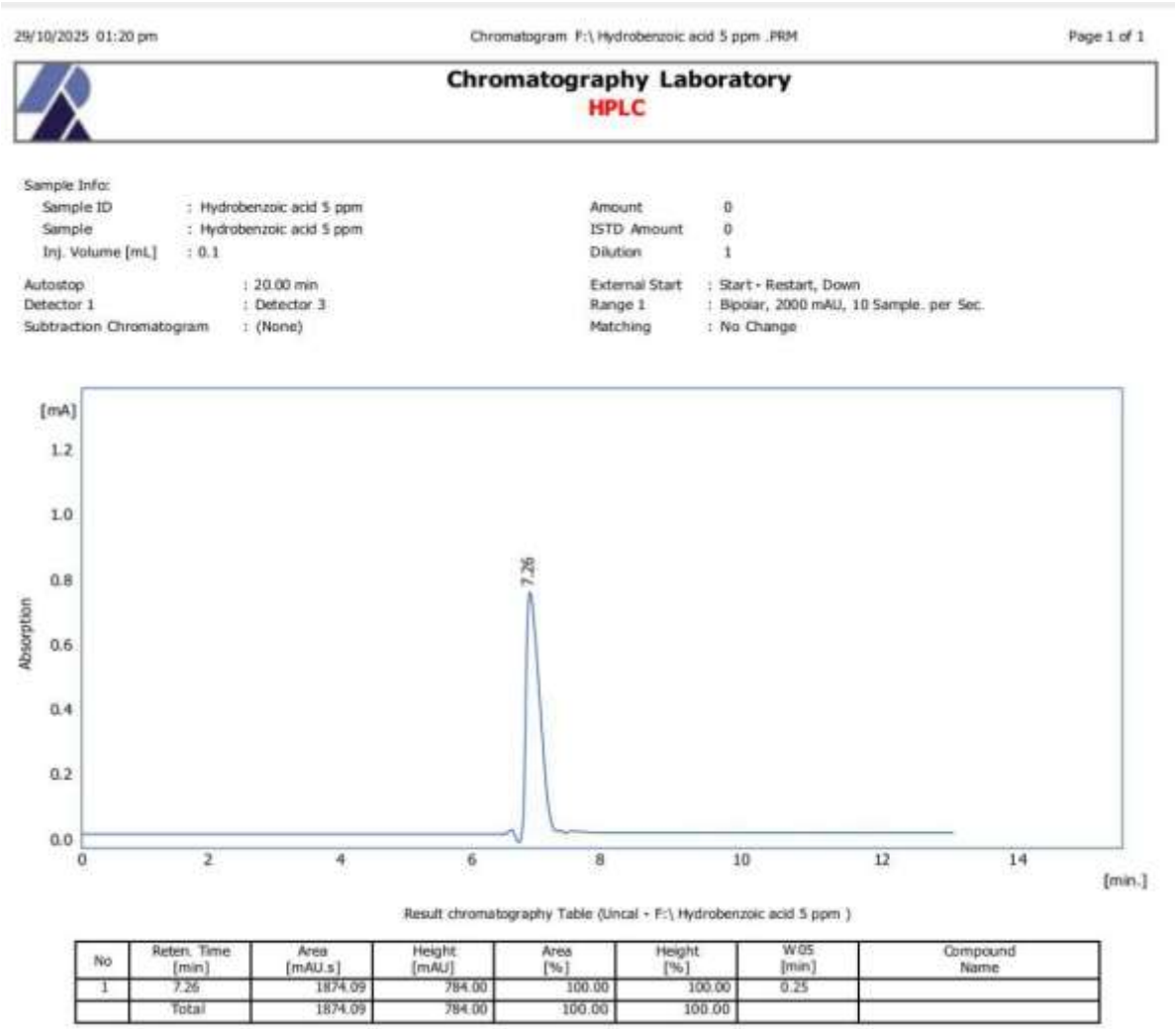

Figure 7.Standard chromatogram Hydrobenzoic acid

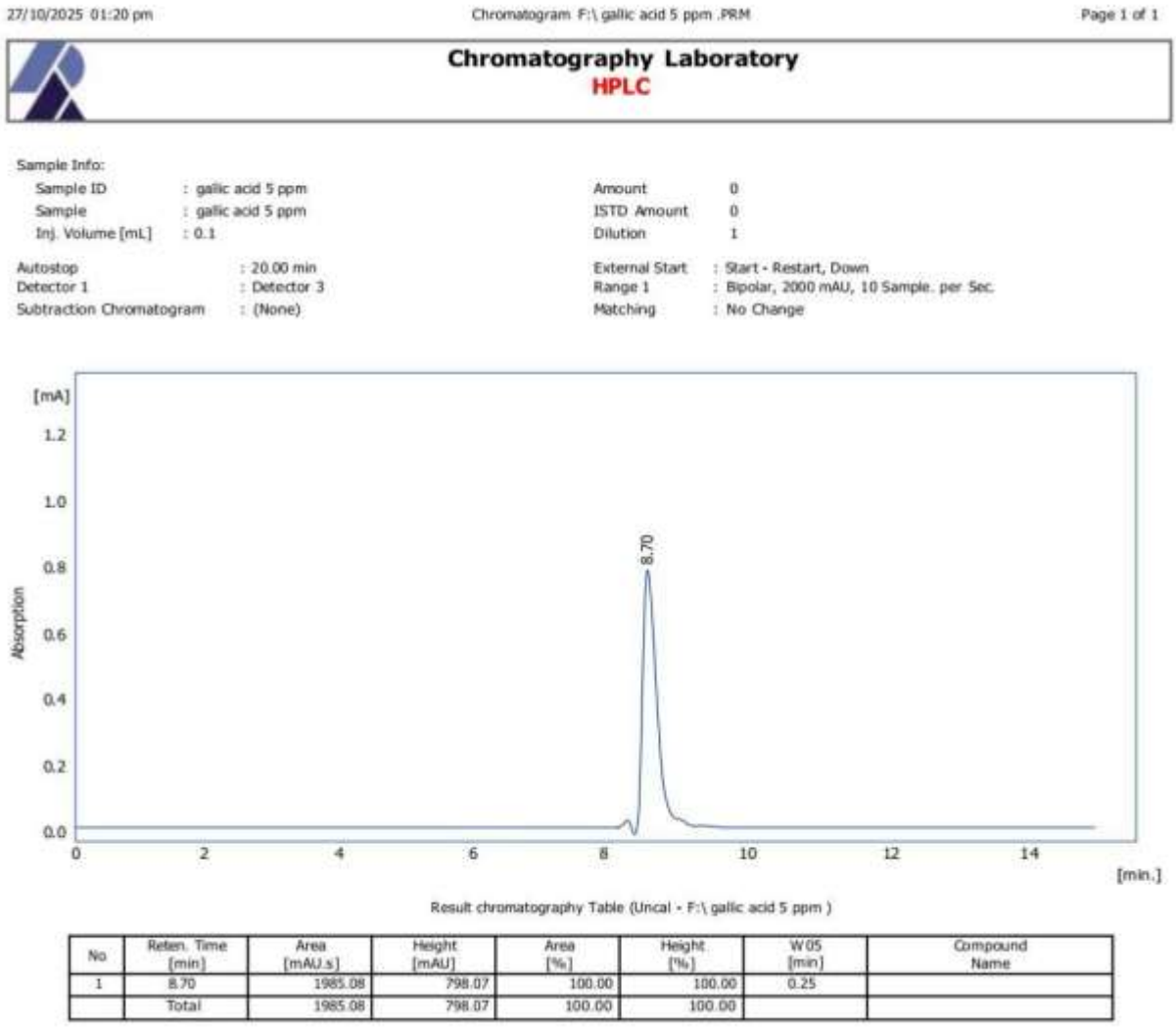

Figure 8. Standard chromatogram Gallic acid

Table (2): Phenolic compounds and their concentrations

No.	Compound Name	Classification	Retention Time (RT, min)	Concentration (µg/mg extract)
1	Caffeic acid	Phenolic acid	3.80	65.9
2	Ferulic acid	Phenolic acid	10.40	92.6
3	Gallic acid	Phenolic acid	8.70	269.8
4	Hydrobenzoic acid	Phenolic acid	7.26	74.0
5	Quercetin	Flavonoid	11.95	198.0
6	Ganoderic acid (A)	Triterpenoid	4.25	485.7
7	Rutin	Flavonoid	5.90	214.9

Spectroscopic Analysis (UV–Vis and FTIR)

The successful green synthesis of ZnO nanoparticles was confirmed through comprehensive spectroscopic and microscopic characterization. The UV–Vis spectrum (Fig. 11) displayed a characteristic surface plasmon resonance (SPR) absorption band with a maximum at 271 nm and additional shoulders at 256.5, 282, 315, and 324 nm, indicative of ZnO nanoparticles with size-dependent quantum confinement effects. The sharpness of the absorption peak suggests a narrow size distribution. FTIR spectroscopy (Fig. 12) confirmed the presence of functional groups from the extract coating on the nanoparticle surface (O–H, C–H, C=O, and C–O stretches) and demonstrated a characteristic Zn–O stretching vibration at 450–550 cm^{-1}, confirming the formation of ZnO.

XRD analysis (Fig. 13) revealed sharp, well-defined diffraction peaks at 2θ values of 31.77°, 34.42°, 36.25°, 47.54°, 56.60°, 62.86°, 66.38°, 67.96°, and 69.10°, which were indexed to the (100), (002), (101), (102), (110), (103), (200), (112), and (201) crystal planes of the hexagonal wurtzite structure of ZnO (JCPDS Card No. 36-1451). The absence of impurity peaks confirmed the high purity of the synthesized nanoparticles. The average crystallite size, calculated using the Debye–Scherrer equation from the most intense (101) peak, was approximately 25 nm.

SEM analysis (Fig. 14) showed that the ZnO nanoparticles exhibited a predominantly quasi-spherical to irregular morphology with a tendency toward aggregation, attributed to the high surface energy and the presence of organic capping agents from the extract. Particle sizes observed by SEM ranged from 55 to 65 nm, representing the size of agglomerated clusters. TEM analysis provided higher resolution, revealing individual nanoparticles with sizes ranging from 15 to 30 nm, confirming the nano-scale dimensions of the synthesized material. The discrepancy between SEM and TEM sizes is typical and reflects the aggregation of primary crystallites into larger secondary particles.

EDX analysis (Fig. 15) confirmed the elemental composition, showing strong signals for zinc (Zn) at 1.0, 8.6, and 9.6 keV and oxygen (O) at 0.5 keV. The absence of other elemental peaks confirmed the purity of the synthesized ZnO nanoparticles. The weight percentages of Zn and O were consistent with the stoichiometric composition of ZnO.

Antifungal Activity: Comparative Efficacy of Ethanolic and Nano-Formulated Extracts
Both the ethanolic extract and the ZnO nano-formulated extract exhibited concentration-dependent antifungal activity against all thirteen mycotoxigenic fungal isolates (Table 3). The ethanolic extract progressively reduced colony diameter from 72.77 mm (control) to 52.69 mm at 0.5 mg/mL and further to 7.85 mm at 2 mg/mL, achieving complete inhibition (100%) at concentrations ≥ 2.5 mg/mL. The inhibition percentages ranged from 27.34% (0.5 mg/mL) to 100% (2.5 mg/mL).

The ZnO nano-formulated extract demonstrated significantly enhanced antifungal efficacy ($P \leq 0.05$). At 0.5 mg/mL, colony diameter decreased to 24.46 mm (66.79% inhibition), which

was significantly greater than the 27.34% inhibition achieved by the crude extract at the same concentration. Notably, complete inhibition (100%) was achieved at concentrations ≥ 1.0 mg/mL for the nano-formulation, compared to 2.5 mg/mL for the crude extract. This represents a 2.5-fold reduction in the effective fungicidal concentration. The enhanced activity can be attributed to: (1) the increased surface area-to-volume ratio of nanoparticles facilitating enhanced interaction with fungal cell surfaces; (2) the synergistic antifungal effects of ZnO (membrane disruption and ROS generation) and the bioactive coating; and (3) improved cellular uptake and sustained release of bioactive compounds [Sirelkhatim et al., 2015; He et al., 2011].

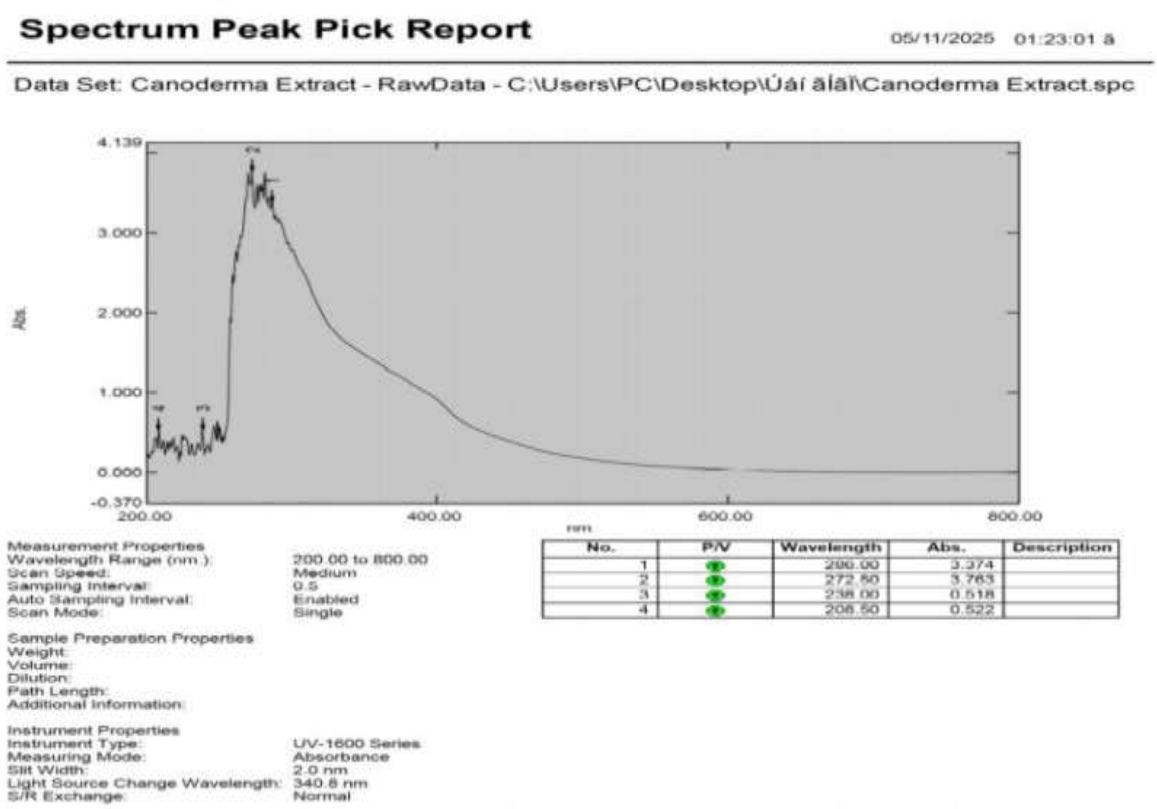

Figure (9): UV-Vis Spectrum of Ethanolic Extract

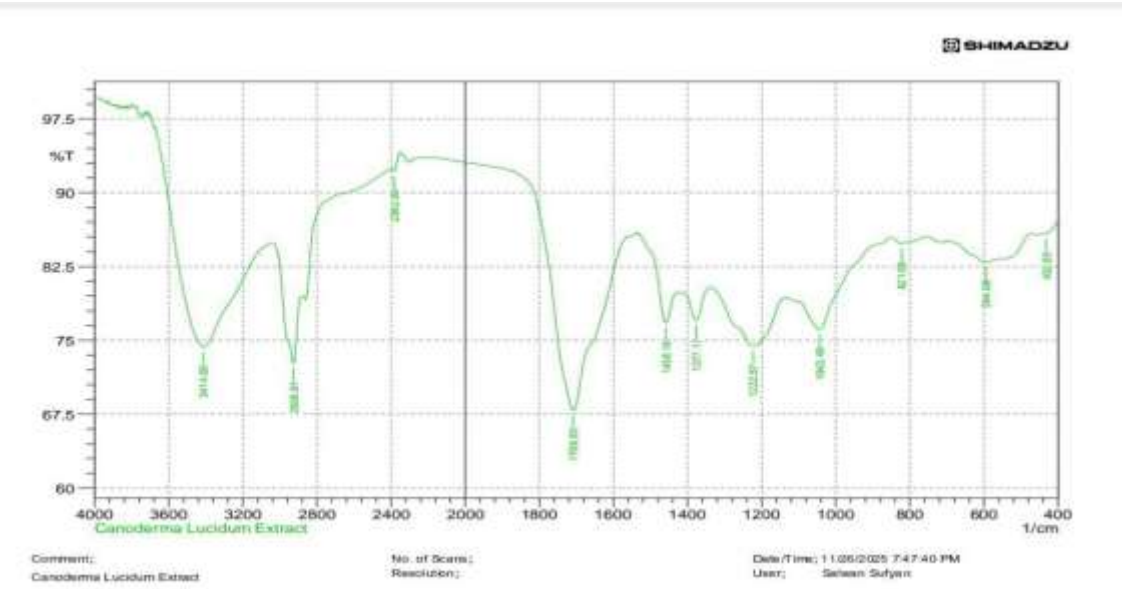

Figure (10): FTIR spectrum of ethanolic extract

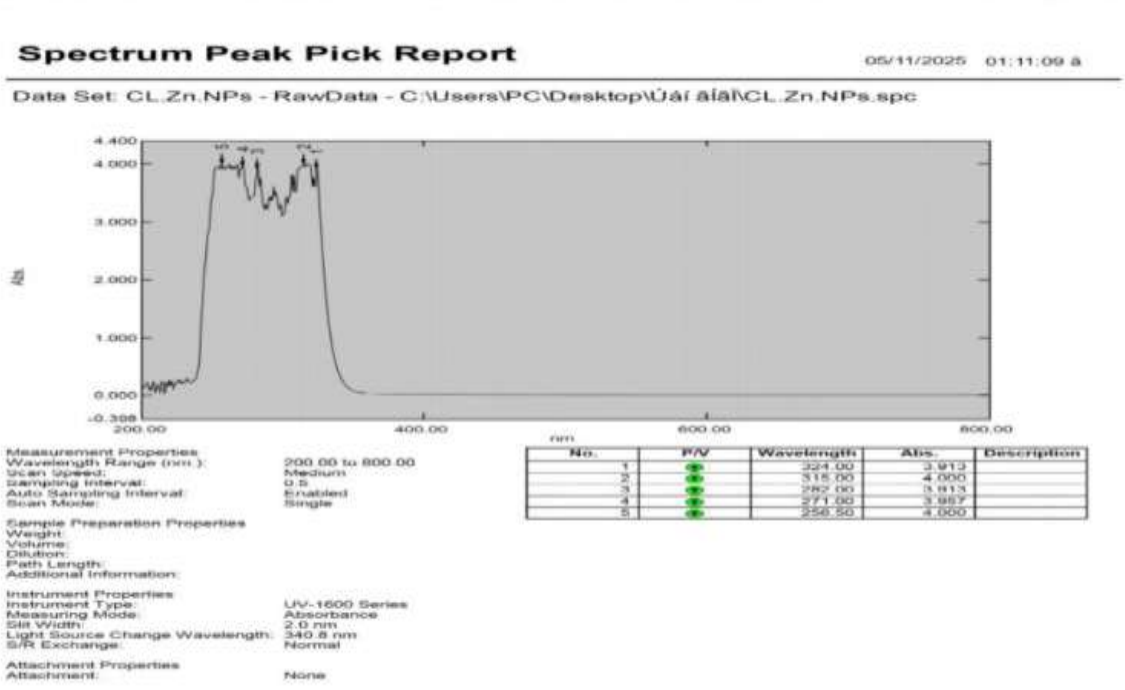

Figure (11): UV–Vis of ZnO nanoparticles

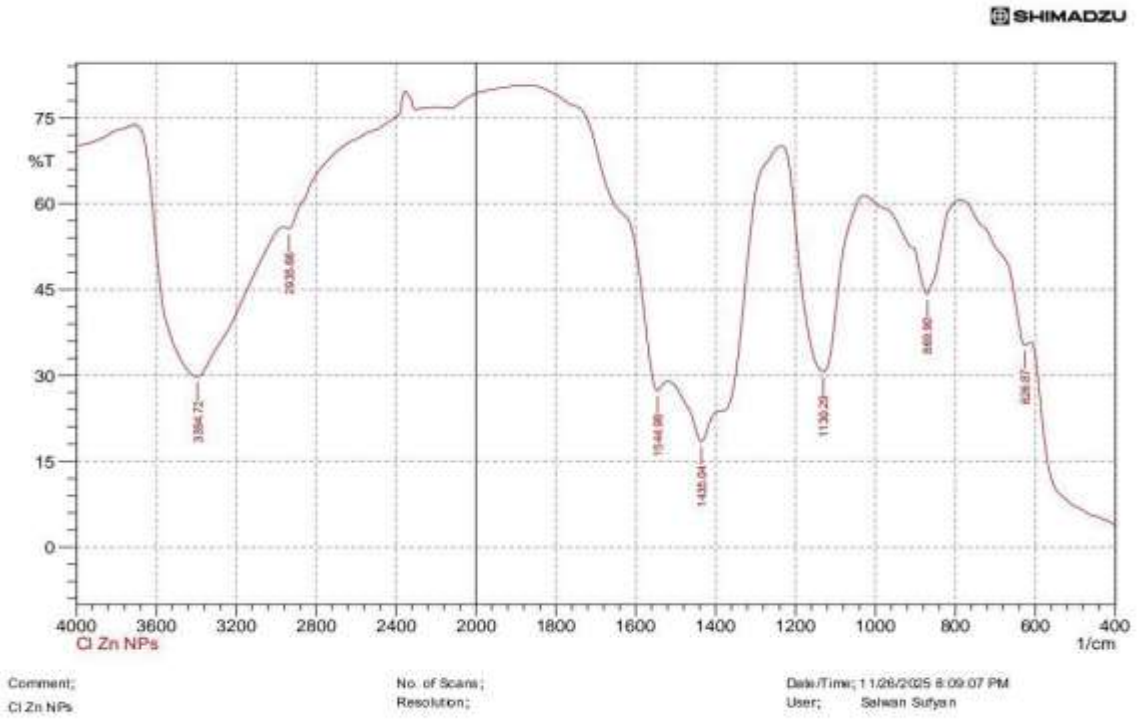

Figure (12): FTIR of ZnO nanoparticles

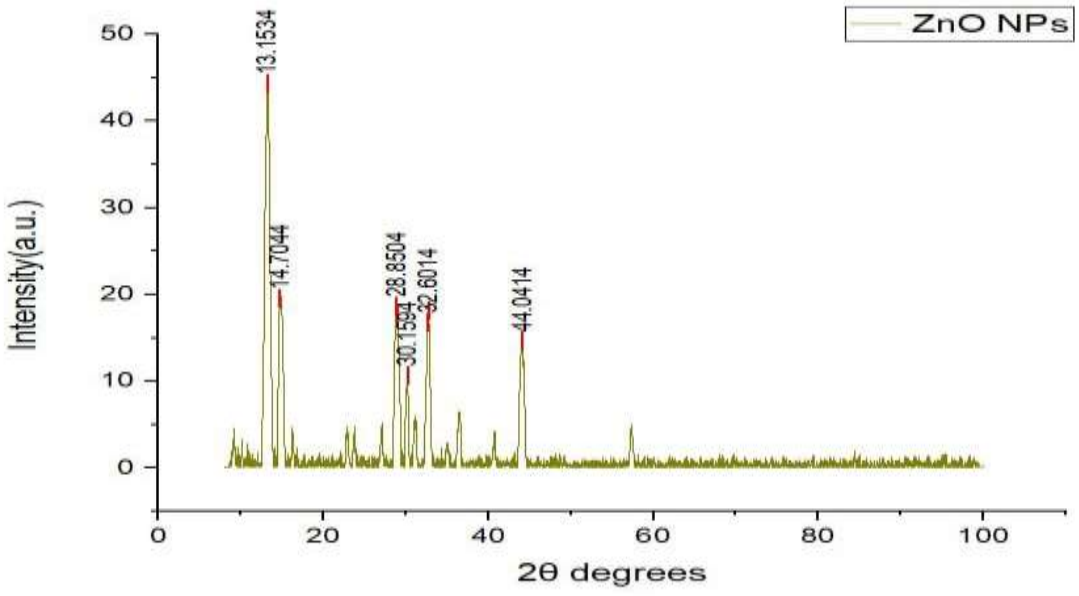

Fig. 13: XRD pattern of ZnO nanoparticles

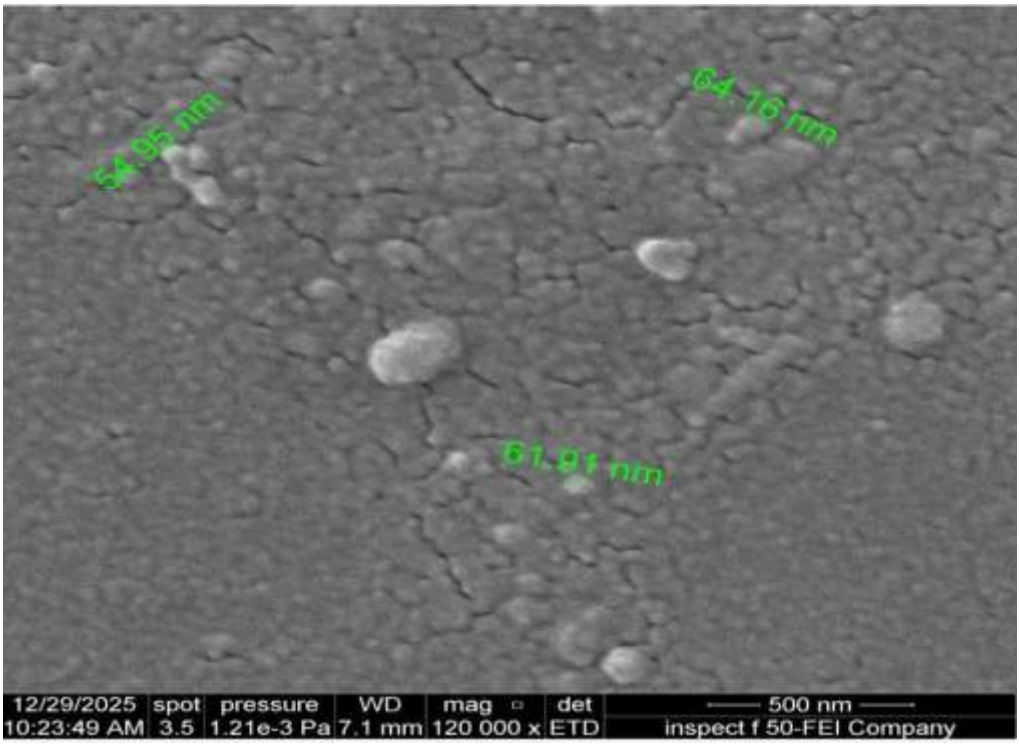

Figure (14): SEM image of nanoparticles

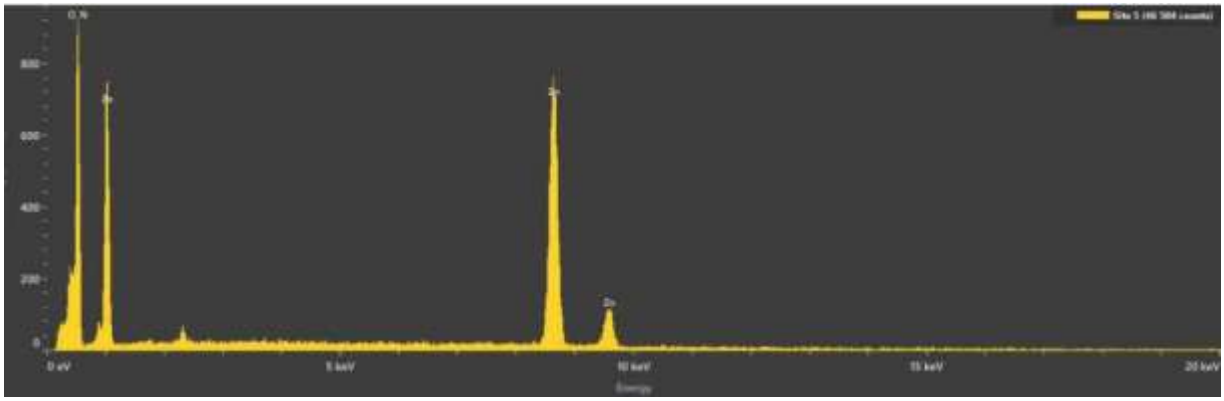

Figure (15): EDX spectrum of nanoparticles

Table 3. Effect of ethanolic and nano-formulated extracts of Ganoderma lucidum on fungal growth (colony diameter, mm) at different concentrations.

ungal Species	Control (mm)	Ethanolic Extract (mg/mL)					Control (mm)	Nano Extract (mg/mL)				
		0.5	1.0	1.5	2.0	2.5		0.5	1.0	1.5	2.0	2.5
Penicillium chrysogenum	75	55	35	20	8	0	75	25	0	0	0	0
Alternaria alternata	73	53	33	18	7	0	73	24	0	0	0	0
Aspergillus oryzae	70	50	30	17	7	0	70	23	0	0	0	0
Aspergillus flavus (A1)	76	56	36	21	8	0	76	26	0	0	0	0
Aspergillus flavus (A2)	75	55	35	20	8	0	75	25	0	0	0	0

Penicillium odoratum	68	48	29	16	6	0	68	22	0	0	0	0
Penicillium thomii	66	47	28	15	6	0	66	21	0	0	0	0
Alternaria porri	72	52	32	18	7	0	72	24	0	0	0	0
Penicillium glabrum	69	49	30	17	7	0	69	22	0	0	0	0
Aspergillus fumigatus	78	58	38	22	10	0	78	30	0	0	0	0
Penicillium citrinum	71	51	32	18	7	0	71	23	0	0	0	0
Fusarium falciforme	77	57	37	21	9	0	77	29	0	0	0	0
Aspergillus versicolor	74	54	34	19	8	0	74	24	0	0	0	0
LSD ($P \leq 0.05$)												

Summary Table – Mean Colony Diameter per Treatment:

Treatment	0.5	1.0	1.5	2.0	2.5
Ethanolic	50.53	40.07	33.31	26.46	21.07
Nano	24.00	0.00	0.00	0.00	0.00

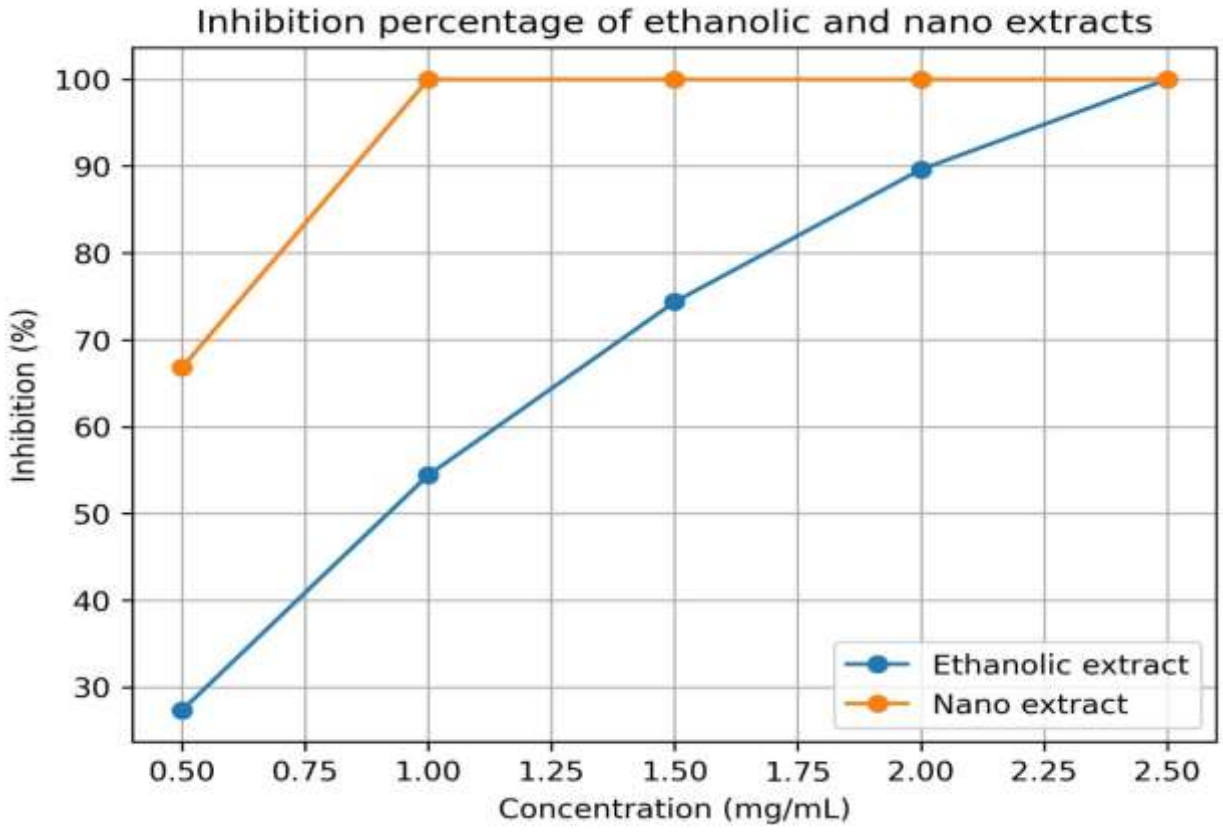

Fig. 16. Inhibition percentage of ethanolic and nano-formulated extracts of *Ganoderma lucidum* against mycotoxigenic fungi at different concentrations.

MIC and MFC Determination

The MIC of the ethanolic extract was 2.0 mg/mL, and the MFC was 2.5 mg/mL (Table 4). In striking contrast, the ZnO nano-formulated extract exhibited significantly lower MIC (0.5 mg/mL) and MFC (1.0 mg/mL) values. The four-fold reduction in MIC and 2.5-fold reduction in MFC provide strong quantitative evidence for the nano-enhancement effect. The MIC/MFC ratio was < 4 for both formulations (1.25 for crude, 2.0 for nano), indicating fungicidal rather than fungistatic activity.

Microscopic Confirmation of Antifungal Mechanisms

Transmission electron microscopy of treated fungal cells revealed distinct ultrastructural alterations. Control hyphae showed intact cell walls, organized cytoplasmic contents, and normal organelle structures. Ethanolic extract treatment resulted in cell wall thinning, membrane irregularities, and cytoplasmic vacuolization. The nano-formulated extract caused more severe damage, including complete cell wall disintegration, plasma membrane rupture, leakage of cytoplasmic contents, and organelle degradation. These observations are consistent with the proposed mechanisms of ZnO nanoparticle-induced oxidative stress and membrane damage [Sirelkhatim et al., 2015].

Antimycotoxigenic Activity Assessed by HPLC

A key objective of this study was to distinguish between growth-dependent and growth-independent inhibition of mycotoxin production. By employing sub-inhibitory concentrations (0.5 × MIC), we ensured that any observed reduction in mycotoxin levels was not merely a consequence of reduced fungal biomass but reflected specific interference with toxin biosynthetic pathways. The HPLC analysis revealed a progressive reduction in aflatoxin B1 levels (Table 6). The control (untreated) culture produced 126.9 ppb of aflatoxin B1. Treatment with the ethanolic extract at 1.0 mg/mL reduced mycotoxin concentration to 52.1 ppb (58.9% reduction) . The ZnO nano-formulated extract at 0.25 mg/mL yielded the most pronounced reduction, with mycotoxin levels decreasing to 15.9 ppb (87.5% reduction compared to control).

The superior antimycotoxigenic activity of the nano-formulation, even at 8-fold lower concentration than the crude extract MIC, suggests specific interference with aflatoxin biosynthesis. Potential mechanisms include: (1) zinc ion-mediated inhibition of key enzymes in the aflatoxin biosynthetic gene cluster, (2) downregulation of regulatory genes (aflR, aflS) by phenolic compounds from the extract, and (3) oxidative stress from ZnO-NPs disrupting the redox-sensitive secondary metabolism [9,10]. The substantial reduction in mycotoxin levels achieved by the nano-formulation highlights its dual functional capability as both an antifungal and antimycotoxigenic agent.

Table 4. Minimum inhibitory concentration (MIC) and minimum fungicidal concentration (MFC) of ethanolic and nano-formulated extracts of *Ganoderma lucidum* against mycotoxigenic fungi

Extract Type	MIC (mg/mL)	MFC (mg/mL)
Ethanolic extract	2.0	2.5
Nano extract	0.5	1.0

Microscopic Observations

Microscopic examination revealed clear morphological alterations in fungal structures following treatment. In the control group, normal fungal growth was observed, characterized by intact conidial heads and dense spore formation. In contrast, treatment with the ethanolic extract resulted in noticeable deformation of fungal structures along with reduced sporulation. The nano-formulated extract caused more pronounced structural alterations, including distortion of conidial heads and disruption of hyphal structures (Fig. 17).

Fungle	Control (mm)	Ethanolic extract (mm/ml)	Nano extract (mg/ml)
Aspergillus flavus			
Penicillium citrinum			
Fusarium falciforme			

Fig. 17. Comparative antifungal activity of ethanolic and nano-formulated extracts of Ganoderma lucidum against selected mycotoxigenic fungi. Control plates exhibit normal growth, whereas ethanolic extract reduces fungal growth and nano-formulated extract shows pronounced inhibition

Mycotoxin Reduction Assessed by HPLC Analysis

The effect of ethanolic and nano-formulated extracts of *Ganoderma lucidum* on mycotoxin production was evaluated using High-Performance Liquid Chromatography (HPLC). The results showed a reduction in mycotoxin levels in treated samples compared to the control. The mycotoxin concentration in the control reached 126.9 ppb, which decreased to 52.1 ppb following treatment with the ethanolic extract. A greater reduction was observed in the nano-formulated extract, where the concentration decreased to 15.9 ppb. The HPLC chromatogram of the control sample (Fig. 18) showed distinct peaks at retention times of approximately 4.07 and 5.95 min, corresponding to mycotoxin compounds. In contrast, the chromatogram of the ethanolic extract (Fig. 19) showed a reduction in peak intensity and area. The nano-formulated extract (Fig. 20) exhibited a more pronounced decrease in peak intensity. Quantitative analysis showed a reduction in mycotoxin levels after treatment (Table 6).

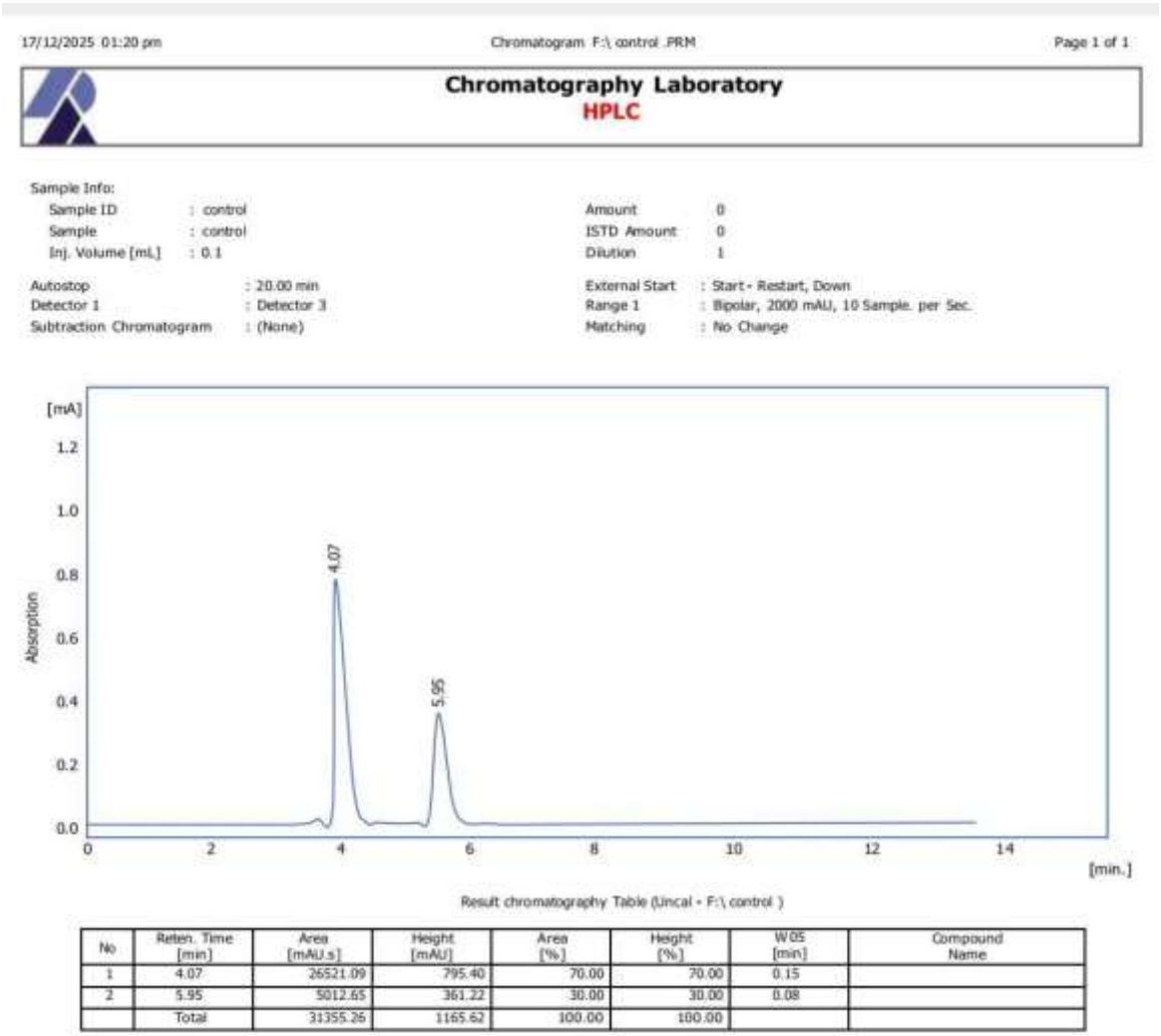

No	Reten. Time [min]	Area [mAU.s]	Height [mAU]	Area [%]	Height [%]	W05 [min]	Compound Name
1	4.07	26521.09	795.40	70.00	70.00	0.15	
2	5.95	5012.65	361.22	30.00	30.00	0.08	
	Total	31355.26	1165.62	100.00	100.00		

Fig. 18. HPLC chromatogram of mycotoxins in control sample.

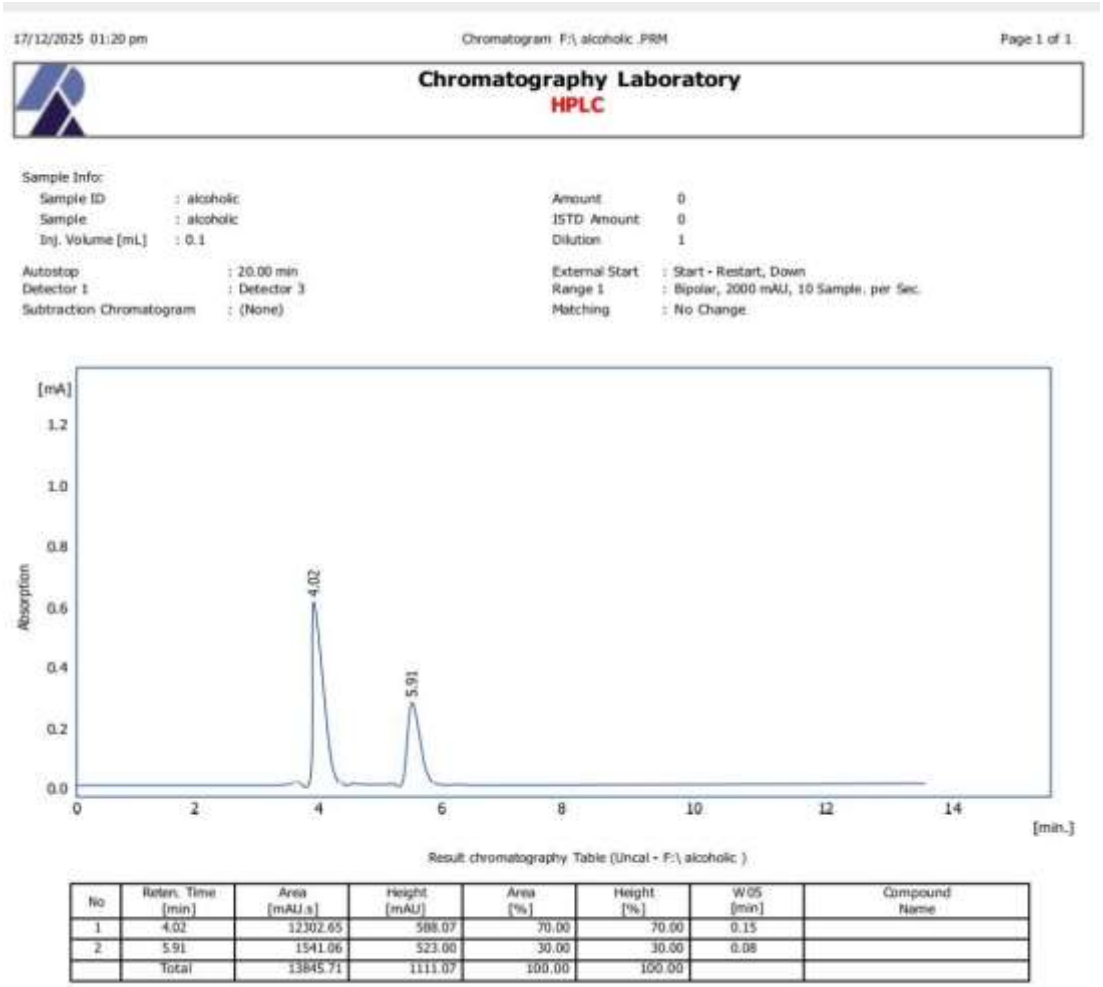

No	Reten. Time [min]	Area [mAU.s]	Height [mAU]	Area [%]	Height [%]	W05 [min]	Compound Name
1	4.02	12302.65	588.07	70.00	70.00	0.15	
2	5.91	1541.06	523.00	30.00	30.00	0.08	
	Total	13845.71	1111.07	100.00	100.00		

Fig. 19. HPLC chromatogram after treatment with ethanolic extract.

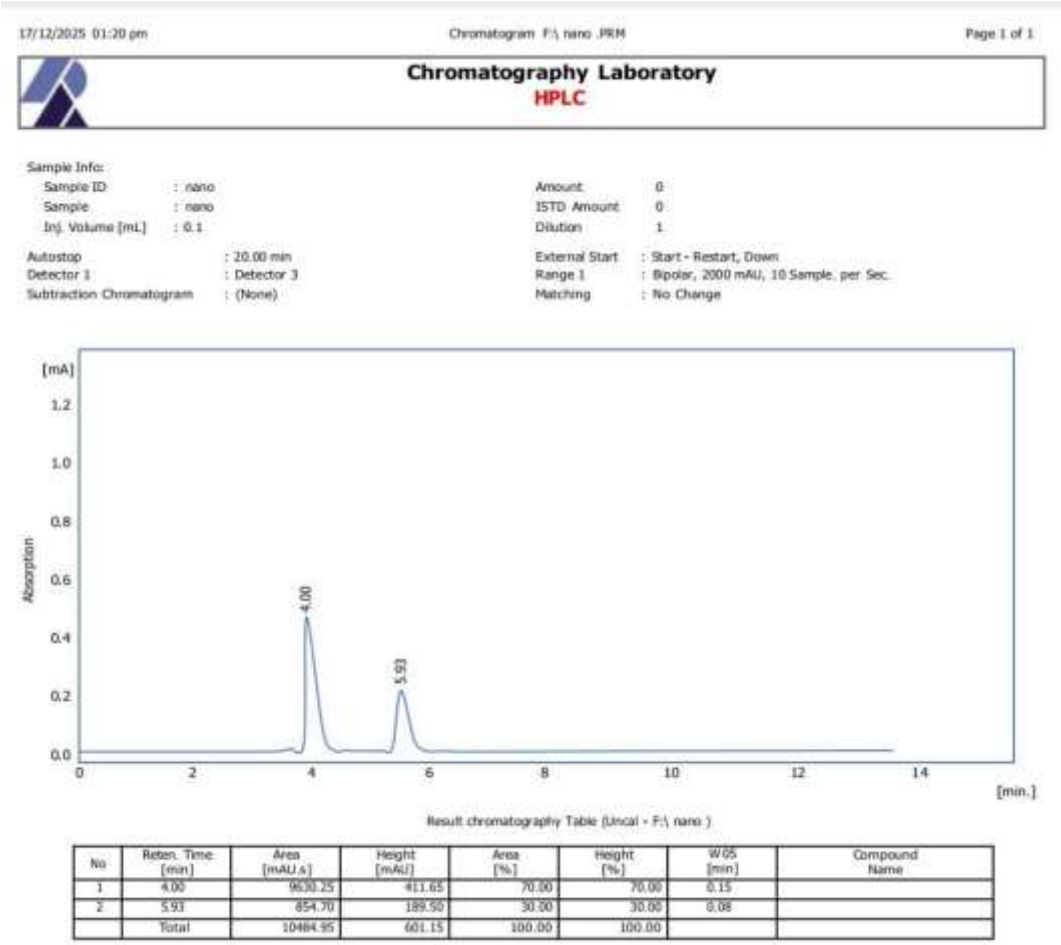

Fig. 20. HPLC chromatogram after treatment with nano-formulated extract.

Quantitative analysis showed a reduction in mycotoxin levels after treatment (Table 6).

Treatment	Mycotoxin concentration (ppb
Control	126.9
Ethanolic extract	52.1
Nano extract	15.9

Table 6. Quantitative analysis of mycotoxin concentration (ppb) in control and treated samples using HPLC.

4-Discussion

The results of the present study demonstrate that both the ethanolic extract and the ZnO nano-formulated extract of *Ganoderma lucidum* possess significant antifungal activity and inhibitory effects on mycotoxin production against a diverse panel of mycotoxigenic fungi. Critically, the nano-formulated extract exhibited markedly higher efficacy across all measured parameters, validating the hypothesis of nano-enhancement.

The antifungal activity of the ethanolic extract can be attributed to the presence of bioactive compounds, particularly phenolic acids, flavonoids, and triterpenoids identified through GC–MS and HPLC analyses. These compounds are known to disrupt fungal cell membranes, increase membrane permeability, and inhibit essential enzymatic systems involved in

fungal metabolism [7]. Ganoderic acid A, the most abundant compound detected (485.7 µg/mg), is a lanostane-type triterpenoid known to interact with ergosterol biosynthesis and membrane integrity, providing a specific mechanistic rationale for the observed antifungal activity.

Several synergistic mechanisms explain the superior performance of the ZnO nano-formulated extract. First, the reduced particle size (15–30 nm by TEM) dramatically increases the specific surface area, enhancing interaction with fungal cells and facilitating the delivery of bioactive compounds. Second, ZnO nanoparticles exert intrinsic membranolytic effects through electrostatic interaction with the negatively charged fungal membrane, causing structural disruption and increased permeability. Third, ZnO nanoparticles generate reactive oxygen species (ROS), including superoxide radicals, hydroxyl radicals, and hydrogen peroxide, which induce oxidative damage to critical cellular macromolecules (proteins, lipids, and nucleic acids). Fourth, zinc ions released from the nanoparticles can interfere with essential metal-dependent enzymes. Finally, the bioactive coating from the extract provides complementary antifungal activity and may facilitate cellular recognition and uptake [8].

Regarding antimycotoxigenic activity, the significant reduction in aflatoxin B1 production at sub-inhibitory concentrations indicates that the treatments interfere specifically with secondary metabolism. The 87.5% reduction achieved by the nano-formulation at 0.25 mg/mL, compared to 58.9% reduction by the crude extract at 1 mg/mL, is particularly noteworthy. This suggests that the nano-formulation components—ZnO and bioactive compounds—may act synergistically to inhibit the aflatoxin biosynthetic gene cluster. Keller [10] described that fungal secondary metabolism is regulated by complex, interconnected gene clusters responsive to environmental cues including oxidative stress. Tian et al. [11] further demonstrated that targeting alternative oxidase and redox homeostasis can effectively disrupt mycotoxin production. The oxidative stress generated by ZnO nanoparticles may thus serve as a signal that downregulates secondary metabolite biosynthesis.

The practical implications of these findings are significant for food safety and agricultural applications. The enhanced potency at lower concentrations suggests that nano-formulated *G. lucidum* extracts could be developed as effective natural preservatives or antifungal treatments, reducing the required dosage and associated costs. However, several important considerations must be addressed before practical application: (1) comprehensive toxicity assessment of the nano-formulation on human cell lines and in vivo models, (2) evaluation of effects on organoleptic properties of treated foods, (3) assessment of environmental impact and ecotoxicity, (4) stability and shelf-life studies under various storage conditions, (5) scalability and cost-effectiveness of green synthesis for commercial production, and (6) compliance with regulatory requirements for nanomaterials in food applications. Future research should also investigate the specific molecular targets using transcriptomic and proteomic approaches, evaluate efficacy in real food matrices, and

explore combination strategies with other natural preservatives [4].

Conflict of Interest

The authors report no conflicts of interest associated with this manuscript.

Author Contributions

All authors contributed equally to the conception, design, and execution of this study. All authors participated in data acquisition, analysis, and interpretation. The first draft of the manuscript was prepared collaboratively, and all authors reviewed and approved the final version for submission.

Data Availability

The datasets generated and/or analyzed during the current study are available from the corresponding author upon reasonable request.

5-References

[1] Eskola, M., Kos, G., Elliott, C. T., Hajšlová, J., Mayar, S., and Krska, R. (2020). Worldwide contamination of food-crops with mycotoxins: Validity of the widely cited "FAO estimate" of 25%. *Critical Reviews in Food Science and Nutrition*, 60(16), 2773–2789.

[2] Ahmad, M. F., Alsayegh, A. A., Ahmad, F. A., and Akhtar, M. S. (2024). *Ganoderma lucidum*: A comprehensive insight into antimicrobial and antioxidant properties with emerging applications. *Heliyon*, 10(2), e24075.

[3] Vahdani, M., Shoeibi, S., and Amini, M. (2022). Effect of different extracts of *Ganoderma lucidum* on ochratoxin A formation by *Aspergillus ochraceus*. *Research Journal of Pharmacognosy*, 9(2), 63–70.

[4] Zhang, L., Cheng, Y., Yang, X., and Li, P. (2023). Application of nanotechnology in mycotoxin control and detoxification in food and agro-food systems. *Critical Reviews in Food Science and Nutrition*, 63(33), 12488–12512.

[5] Azwanida, N. N. (2015). A review on the extraction methods use in medicinal plants: Principle, strength and limitation. *Medicinal & Aromatic Plants*, 4(3), 196.

[6] Ramesh, M., Anbuvannan, M., and Viruthagiri, G. (2015). Green synthesis of ZnO nanoparticles using *Solanum nigrum* leaf extract and their antibacterial activity. *Spectrochimica Acta Part A: Molecular and Biomolecular Spectroscopy*, 136, 864–870.

[7] Rašeta, M., Mišković, J., Čapelja, E., Zaporozhanets, T., Karaman, M., and others (2023). Do *Ganoderma* Species Represent Novel Sources of Phenolic-Based Antimicrobial Agents? *Molecules*, 28(7), 3264.

[8] Sirelkhatim, A., Mahmud, S., Seeni, A., Kaus, N. H. M., Ann, L. C., Bakhori, S. K. M., Hasan, H., and Mohamad, D. (2015). Review on zinc oxide nanoparticles: antibacterial activity and toxicity mechanism. *Nano-Micro Letters*, 7(3), 219–242.

[9] He, L., Liu, Y., Mustapha, A., and Lin, M. (2011). Antifungal activity of zinc oxide nanoparticles against *Botrytis cinerea* and *Penicillium expansum*. *Journal of Applied Microbiology*, 111(2), 461–469.

[10] Keller, N. P. (2019). Fungal secondary metabolism: regulation, function and drug discovery. *Nature Reviews Microbiology*, 17(3), 167–180.

[11] Tian, F. (2020). Alternative Oxidase: A Potential Target for Controlling Fungal Pathogens. *Frontiers in Microbiology*, 11, 419.